

Low energy cluster beam deposition technique: Development and deposition of cluster assembled Sb thin films

G. V. Ravi Prasad*, B. K. Patel*, S. Chakravarty*, R. Mythili**, M. Vijaylakshmi**, B. R. Sekhar*, S. N. Sahu*[†], V. S. Ramamurthy[§] and S. N. Behera*

*Institute of Physics, Sachivalaya Marg, Bhubaneswar 751 005, India

**Physical Metallurgy Section, Material Characterization, Indira Gandhi Center of Atomic Research, Kalpakkam 603 102, India

[§]Department of Science and Technology, Technology Bhavan, New Mehrauli Road, New Delhi 110 016, India

Antimony cluster thin films have been synthesized by the newly-developed low energy cluster beam deposition technique. Proton-induced X-ray emission analysis shows absence of any foreign impurity even at ppm level. Structural analysis by glancing angle X-ray diffraction indicates presence of rhombohedral Sb along with Sb-oxides. Transmission electron microscopy micrographs for 20 Å and 100 Å films respectively show the size distribution along with isolated aggregates. The size distribution for 100 Å thick film is found to be large compared to the 20 Å one. Transmission electron diffraction studies reveal hexagonal symmetry.

RECENTLY there has been considerable interest in the study of cluster and cluster-assembled nanomaterials because of their novel properties¹ and technological applications². Cluster-generated solids differ from both the amorphous and crystalline structures in the sense that the short range order in them is controlled by the grain size and long range order does not exist due to random stacking of nano grains. A high quality well crystallized film can be realized by currently available cluster deposition technique. Of various cluster deposition techniques²⁻⁸, low energy cluster beam deposition (LECBD) methods⁹⁻¹³ are attractive. Neutral clusters can be generated either by laser ablation⁷ or by thermal evaporation⁹⁻¹³ followed by inert gas condensation. Cluster size can be determined by mass analysis through a time of flight (TOF)⁹⁻¹⁴ mass spectrometer measurement. Typical cluster size can range from a few tens to a few thousand atoms. In this method the nucleation of clusters is achieved by gas condensation process by allowing an inert gas to flow in a cooled environment. Further cooling of the clusters to reduce their kinetic energy is achieved by supersonic expansion. Thus, clusters with very low kinetic energy soft land on the

substrate without fragmentation resulting in the growth of a nanostructured film through a process of coalescence.

The present work describes the development of a LECBD facility at Institute of Physics, Bhubaneswar. In order to test the setup for generation and deposition of clusters, Sb clusters were produced and deposited on various substrates and characterized by performing different measurements. The reason for choosing Sb as a candidate material are (i) its low melting point ($T_m = 260^\circ\text{C}$); (ii) its existence in amorphous state¹¹, (iii) its use as a material for III-V compound semiconductors and (iv) its evaporation in tetrameric form¹⁵. Fabrication of the facility is based on a French design.

The schematic diagram of the LECBD setup is shown in Figure 1 a. Mainly it consists of a source, and a deposition chamber along with TOF arm. The cluster source is a Sattler type¹³ thermal source mounted on a flange on one side of the source chamber. The source can be slid over two metallic arms of the source chamber to facilitate the loading of materials for evaporation. The thermal source consists of a molybdenum crucible with a 3 mm hole facing the deposition chamber. Two heaters, one at the bottom of the crucible and the other at the top cover lid are attached in order to raise the temperature of the crucible up to 1100°C . A radiation heat shield made up of tantalum with an aperture facing the deposition chamber surrounds the crucible to avoid heat loss. The source is connected to a tubular structure made of copper at the end of which, nozzles with different diameters (~ 2 to 5 mm) can be attached. The copper tube along with the nozzle is cooled by liquid nitrogen as shown schematically in Figure 1 b. Inert gases such as He or Ar are allowed to flow at the inlet of the source chamber which push the thermally evaporated atom vapour across the heat shield to the cooled tubular structure for nucleation and cluster growth. The cooled atomic vapour along with the inert gas (in the present case He) undergoes supersonic expansion as it comes out of the nozzle leading to the formation of larger clusters. A conical skimmer separating the source and the deposition chambers helps to maintain the pressure gradient between the two and also collimates the cluster beam there by directing the beam to fall on the substrate in the deposition chamber. A diffstack pump with a pumping speed of 2000 l/s is used to evacuate the source chamber. The deposition and source chambers are evacuated and maintained at typical vacuum of $\approx 1.33 \times 10^{-7}$ mbar and $\approx 1.33 \times 10^{-6}$ mbar respectively. However, when the inert gas (He) flow is initiated, the vacuum of the source chamber deteriorates to about $\approx 1.33 \times 10^{-5}$ mbar. The deposition chamber carries a rotating substrate holder to mount the substrates that can be used to prepare many samples without breaking the vacuum. A quartz crystal thickness monitor placed in the deposition chamber measures the rate of cluster deposition and hence the thickness of the deposited film.

[†]For correspondence. (e-mail: sahu@iopb.res.in)

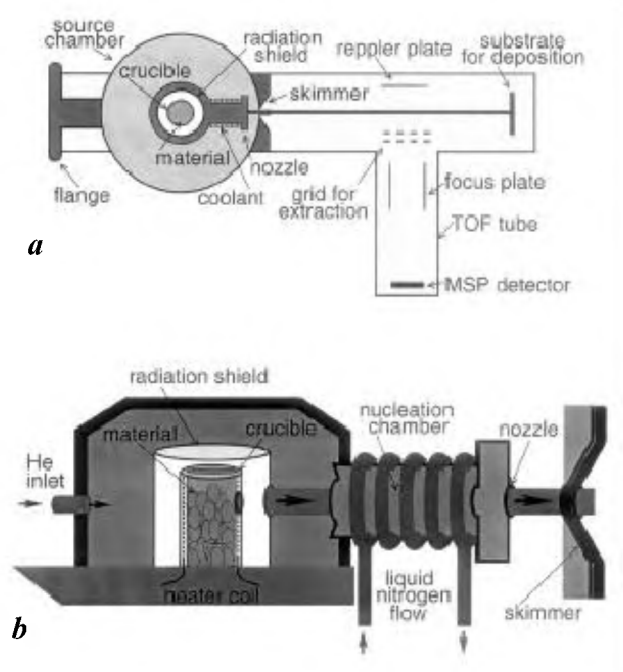


Figure 1. Schematic diagram of the experimental set-up of low energy cluster beam deposition technique. *a*, Top view; *b*, details of cluster source.

In order to deduce the size distribution of the atomic clusters produced by the cluster generator, it is essential to mass analyse them using a TOF mass spectrometer. However, the results reported in this paper are based on mass-unanalysed antimony cluster deposited films. A time of flight set up is under development for mass analysis in future.

In order to produce cluster deposited films of antimony (Sb), the cluster source and the nozzle in the source chamber are aligned using a laser beam, with the skimmer and the substrate in the deposition chamber. The chemically pure antimony ingot is loaded in the crucible and temperature is optimized at 650°C to achieve a reasonable rate of deposition. Increasing the crucible temperature higher than the optimized value results in the loss of material due to quick evaporation whereas at lower temperatures, enough vapour pressure is not generated to achieve a reasonable rate of deposition. The other parameters crucial to the generation of clusters and controlling their size are the pressure of helium flow and the nozzle diameter. On decreasing the size of the nozzle it is expected that the size of the atomic cluster will increase because of the adiabatic expansion and subsequent cooling of the vapour. Similarly the helium flow pressure helps in thermalizing the vapour, which in turn facilitates the nucleation and growth of the cluster. At the same time the helium flow also helps to direct the cluster beam through the nozzle and the skimmer to the deposition chamber. For the Sb deposition the nozzle diameter and the helium pressure are optimized to 3 mm and 5 mbars respectively; which

resulted in a steady deposition rate of 0.1 Å/s; as detected by the thickness monitor, while the Sb vapour got deposited mostly on the inner side of the tantalum heat shield, presumably due to the back flow caused by the increased helium pressure. Antimony clusters thus generated were deposited on different substrates such as glass, silicon and carbon-coated copper grid to facilitate optical absorption, X-ray diffraction and TEM measurements.

In order to see coalescence effect and its influence on the structure and optical properties of Sb-cluster assembled materials we have synthesized films of two different thicknesses, i.e. 20 Å and 100 Å. The samples were characterized using different tools.

As there are only a small number of atoms in a cluster, presence of the smallest amount of impurity atoms may influence its properties dramatically. Hence, to determine the presence of any impurity in the Sb cluster deposited films on the Si substrate, Proton Induced X-ray Emission (PIXE) analysis was carried out using the 3.07 MeV proton beam from 3 MV pelletron accelerator at IOP. The PIXE spectrum of the silicon substrate is shown in Figure 2*a*; while Figure 2*b* shows the spectrum of the 100 Å thick Sb-cluster deposited film on the Si substrate. Additional peaks corresponding to Sb were detected as can be seen in Figure 2*b* when the sample was bombarded with the proton beam for a larger period of time compared to that of the spectrum in

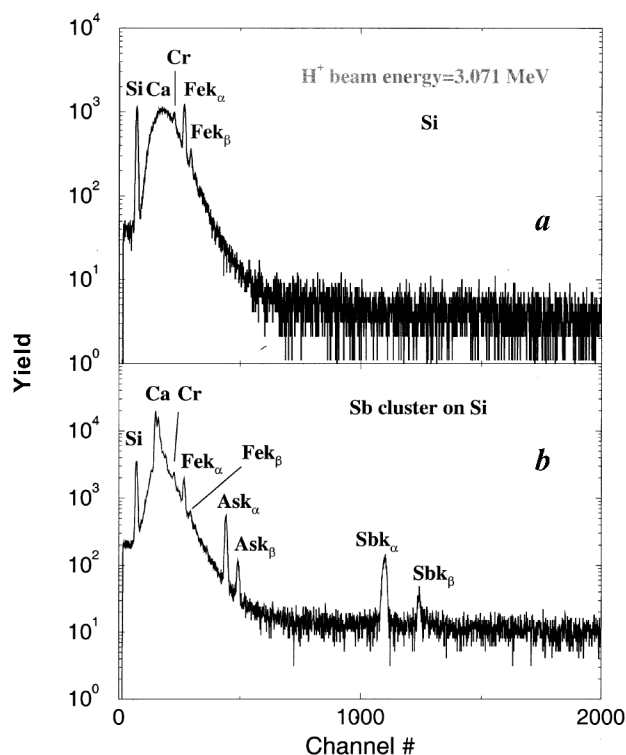


Figure 2. The PIXE spectrum of the silicon substrate (*a*), and the Sb-cluster deposited films on Si-substrate (*b*).

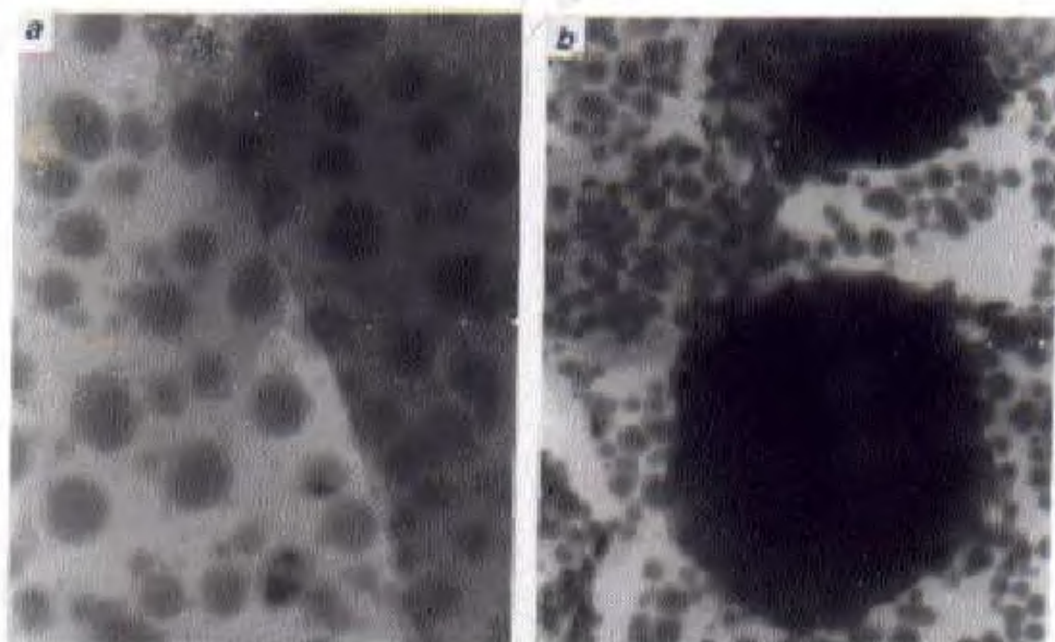


Figure 3. Bright field images of Sb cluster films of thickness (a) 20 Å and (b) 100 Å.

Figure 2 *a*. On bombarding the sample with protons, all the atoms in the sample get excited and emit their characteristic X-rays which can be detected by a Si:Li detector. As a result, the PIXE measurement acquires a sensitivity of detecting trace element impurities present in a sample up to ppm level. Unfortunately the Si:Li detector used in PIXE measurement cannot detect the low Z ($Z < 11$) elements (Z is the atomic number). Hence, presence of low Z impurities such as *O* and *C*, etc. in the deposit cannot be ruled out. Thus, while the presence of Sb has been identified, no other foreign impurities even at ppm level could be detected. Unprotected Sb clusters are highly reactive and prone to oxidation¹⁷ when exposed to ambient atmosphere. Hence, the presence of Sb-oxide in the Sb-cluster deposited films is expected which cannot be detected by PIXE. In order to detect the presence of antimony oxides in the film it is necessary to carry out X-ray diffraction and transmission electron diffraction (TED) measurements. The preliminary results of glancing angle diffraction measurements indeed show the Sb oxidation, which is being analysed at present. The bright field (BF) image transmission electron micrograph (TEM) of 20 Å thick cluster deposited Sb film on carbon coated Cu grid is shown in Figure 3 *a*. Presence of isolated nearly spherical particulates with scattered coagulation events are clearly seen. The size of the crystalline (dark contrast) particulates varies in the range from 16 to 45 nms, implying a large size distribution. It can further be noted that one end of the sample has a shaded or low opacity feature indicating the deposition and growth of one

layer on the other. Figure 3 *b* shows the BF image of the 100 Å thick cluster film deposited on carbon-coated Cu grid. Interestingly the spherical isolated particle feature is completely lost in some region of the film, giving predominantly a coagulation feature having a large surface coverage. Some regions of the sample are completely opaque, suggesting a more prominent aggregation effect. However, the coagulated particles are still isolated but not as much as in the case of 20 Å thick cluster deposited film. Such a feature suggests that increasing the thickness of the deposited cluster film increases the coagulation. The selected area electron diffraction pattern of the 20 Å film is shown in Figure 4 *a* and that for 100 Å thick film is shown in Figure 4 *b*. Characteristic hexagonal symmetry with single crystalline features are exhibited by the samples. However, the streaking in Bragg spots as seen with 100 Å sample (Figure 4 *b*) is totally absent for the 20 Å film, suggesting the presence of one crystalline over the other and more coagulation for 100 Å film compared to that of the 20 Å one. Apart from the Sb phase in the deposit, Sb₂O₃ phase is also detected both for 20 Å and 100 Å films. However, the Sb₂O₃ phases are found to be predominant with 20 Å compared to 100 Å one. Our preliminary results of X-ray diffraction (XRD) analysis also indicate the presence of both Sb and Sb₂O₃ phases in the sample. As we have transferred the samples in air, presence of Sb-oxide in the Sb cluster films is expected.

The lattice spacing values calculated for the 100 Å cluster films are found to be comparable to those of the bulk Sb whereas for that of the 20 Å one the value is

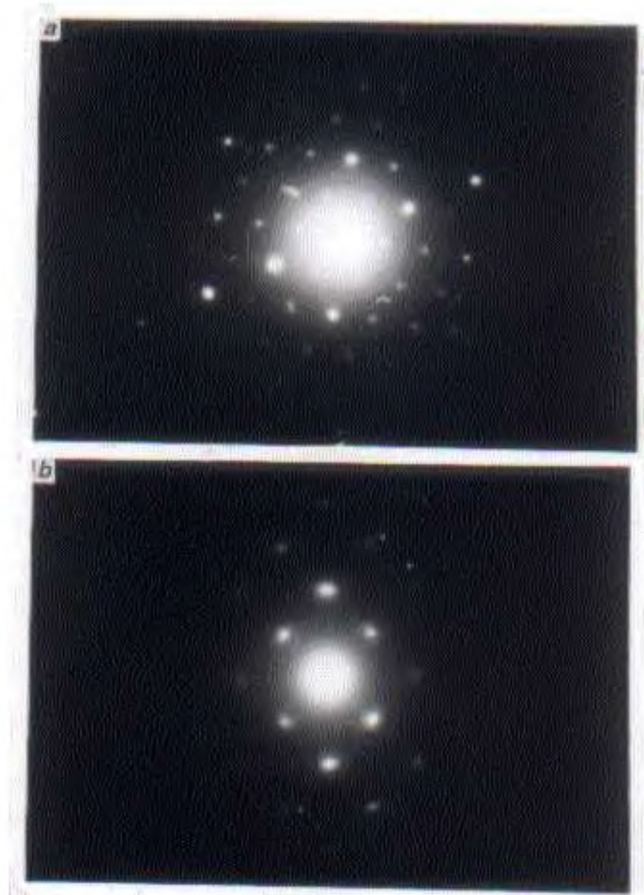


Figure 4. Selected area diffraction patterns of Sb cluster deposited films of thickness (a) 20 Å and (b) 100 Å.

slightly less. The wide diffraction rings as observed in the diffraction pattern suggest that the crystallites are small or amorphous. The size distribution of the particulates in the TEM micrograph of the 100 Å thick Sb-cluster deposited film ranges from 22 to 70 nm (Figure 3b) suggesting the sizes to be larger for the 100 Å thick film compared to the 20 Å one. In fact, in the thicker film large crystallites have grown at the expense of smaller ones.

Photoluminescence (PL) spectrum of the 100 Å thick Sb cluster deposited film taken at 300 K and excited by the radiation of wavelength 411 nm from a Hg–Xe lamp is shown in Figure 5. It shows two red shifted bands around 814 and 893 nm and a blue shifted band around 514 nm. The strong peak at 822 nm is the second harmonic of the exciting radiation. Antimony in the bulk form is a semimetal and is not expected to exhibit photoluminescence. Therefore, the observation of peaks in the photoluminescence spectrum of these cluster assembled films stands testimony to the fact that on deposition the Sb-clusters retain their characteristics and thereby differ from a thin film produced by the standard technique. The appearance of two red-shifted bands in this cluster assembled film could be attributed to the

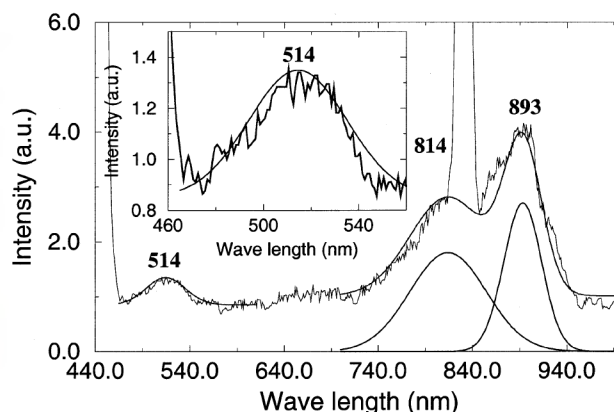


Figure 5. The photoluminescence (PL) spectrum of the 100 Å thick Sb-cluster deposited film on a glass substrate.

trap states generated by off-stoichiometric Sb-oxides, which are expected to be present because of surface oxidation. The blue shifted peak may be attributed to the HOMO–LUMO transition associated with the Sb clusters. These conjectures can be confirmed by performing XRD measurements, which can detect the presence of oxides of antimony. These and other measurements such as Raman scattering and X-ray photoelectron spectroscopy have been performed and are currently being analysed. This will be the subject matter of a future publication.

A low energy cluster beam deposition facility has been developed at Institute of Physics. The 100 Å thick Sb-cluster deposited films show more aggregation effect compared to the 20 Å Sb-cluster films. The TEM micrographs and diffraction patterns show a size distribution and hexagonal symmetry with single crystalline feature. The size of the clusters is found to be larger in the 100 Å thick film compared to that in the 20 Å thick sample.

1. Melinon, P., Pailard, V., Dupuis, V., Perez, A., Jensen, P., Hoareau, A., Perez, J. P. and Tuailon, J., *Int. J. Mod. Phys.*, 1995, **B9**, 339.
2. Nozaki, S., Sato, S., Ono, H., Morisaki, H. and Iwase, M., *Nucl. Instr. Math. Phys. Res.*, 1997, **B121**, 455.
3. Maruno, S., Fujita, S., Watanabe, H., Kusumi, Y. and Ichikawa, J., *Appl. Phys.*, 1998, **83**, 205.
4. Yamada, I., Inokawa, H. and Takagi, T., *J. Appl. Phys.*, 1984, **56**, 2746.
5. Kanayama, T. and Murakami, H., *J. Vac. Sci. Technol.*, 1997, **B15**, 2882.
6. Heiz, U., Vayloyan, A. and Schumacher, E., *Rev. Sci. Instrum.*, 1997, **68**, 3718.
7. Yamamuro, S., Sumiyama, K. and Suzuki, K., *J. Appl. Phys.*, 1997, **85**, 483.
8. Siekmann, H. R., Luder, C., Fachmann, J., Lutz, H. O. and Meiwes-Broer, K. H., *Z. Phys.*, 1991, **D20**, 417.
9. Perez, A., Melinon, P., Dupuis, V., Jensen, P., Prevel, B., Tuailon, J., Bardotti, L., Martet, C., Treilleux, M., Broyer, M., Pellarin, M., Vaille, J. L., Palpant, B. and Lerme, J., *J. Phys. D: Appl. Phys.*, 1997, **30**, 709.

RESEARCH COMMUNICATIONS

10. Fuchs, G., Treilleux, M., Santesh Aires, F., Melinon, P., Cabaud, B. and Hoareau, A., *Thin Solid Films*, 1997, **204**, 107.
11. Fuchs, G., Melinon, P., Santos Aires, F., Treilleux, M., Cabaud, B. and Hoareau, A., *Phys. Rev.*, 1991, **B44**, 3926.
12. Besson, D., Bardotti, L., Hoareau, A., Prevel, B., Treilleux, M. and Esnouf, C., *Mater. Sci. Eng.*, 1997, **B60**, 51.
13. Sattler, K., Muhlbach, J. and Recknagel, E., *Phys. Rev. Lett.*, 1980, **45**, 821.
14. Fuchs, G., Treilleux, M., Santos, F., Cabaud, B., Melinon, P. and Hoareau, A., *Phys. Rev.*, 1991, **A40**, 6128.
15. Resenblatt, G. H. and Lee, P. K., *Chem. Phys.*, 1970, **52**, 1454.
16. Wiley, W. C. and McLaren, I. H., *Rev. Sci. Instrum.*, 1955, **26**, 1150.
17. Fuch, G., Treilleux, M., Santos Aires, F., Cabaud, B., Melinon, P. and Hoareau, A., *Philos. Mag.*, 1991, **63**, 715.

ACKNOWLEDGEMENTS. We thank A. Perez and his group from Universit   Claude Bernard at Lyon, France for their help with the designing of the LECBD set-up. The help of Ph. Cahuzac, and his group from Laboratoire Aime Cotton at Orsay, France is gratefully acknowledged for the fabrication of the Sattler Source. Technical support received from R. C. Nayak and S. C. Choudhury, Institute of Physics, Bhubaneswar with the assembling of the equipment is gratefully acknowledged. Financial support received from IFCPAR through the project No. 1508-4 is gratefully acknowledged.

Received 8 May 2000; revised accepted 8 December 2000
